Climatological Basin-Scale Amazonian Evapotranspiration Estimated through a Water Budget Analysis

HANAN N. KARAM AND RAFAEL L. BRAS

Department of Civil and Environmental Engineering, Massachusetts Institute of Technology, Cambridge, Massachusetts

(Manuscript received 2 February 2007, in final form 13 March 2008)

ABSTRACT

Spatially averaged evapotranspiration [ET] over the Amazon Basin is computed as the residual of the basin's atmospheric water balance equation, at the monthly time scale and for the period 1988–2001. Basin-averaged rainfall [*P*] is obtained from the Global Precipitation Climatology Project (GPCP) dataset, and alternative estimates of the net convergence of atmospheric water vapor flux over the basin [*C*] are derived from three global reanalyses: the NCEP–NCAR and NCEP–Department of Energy (DOE) reanalyses and the 40-yr ECMWF Re-Analysis (ERA-40). Additionally, a best estimate of [*C*] is obtained by taking a weighted average of data from these three sources, in which the weight factors are based on the random error attributed to each reanalysis' [*C*] estimates by comparison to river discharge data. The resulting time series is dominated by ERA-40's contribution, which was found to be the most accurate over the study period. Data products from the three reanalyses are also employed to compute the monthly tendencies of total precipitable water over the basin. While the seasonal signature of this "accumulation term" provides important insight into the Amazon Basin's hydrological cycle, its magnitude is found to be negligible relative to the other components of the water budget. The value of mean annual [ET] presented in this work is significantly lower than other published estimates that are based on simulations by various land surface models. Furthermore, when the best estimate of [*C*] is used, the resulting [ET] time series exhibits a seasonal cycle that is in phase with that of basin-averaged surface net radiation, suggesting that Amazonian evapotranspiration is prevalently limited by energy availability. In contrast, most land surface models, including that of the NCEP–NCAR reanalysis, simulate water-limited evapotranspiration in the Amazon Basin. The analysis presented here supports the hypothesis that most Amazonian trees sustain elevated evapotranspiration rates during the dry season through deep roots, which tap into large reservoirs of soil water that are replenished during the following wet season.

1. Introduction

A recent paper by Werth and Avissar (2004) highlights our poor understanding of evapotranspiration in the Amazon Basin. The authors show that the annual cycles of basin-averaged evapotranspiration simulated by the Goddard Institute for Space Studies (GISS) GCM, the National Centers for Environmental Prediction–National Center for Atmospheric Research (NCEP–NCAR) reanalysis, and the National Aeronautics and Space Administration Goddard Earth Observing System (NASA GEOS) reanalysis diverge in their means, amplitudes, and phases. Additionally, they compare these models with a canopy water balance model developed by Shuttleworth (1988) based on field observations in an old growth forest near Manaus, Brazil. While the GCM and both reanalyses simulate a decline in evapotranspiration during the Amazonian dry season, the Shuttleworth model produces a basin-averaged evapotranspiration cycle that closely tracks that of net radiation, peaking during the dry season when cloudiness is at a minimum. In this latter model, the water stress experienced by Amazonian trees during the dry season is much weaker than in the other land surface schemes, leaving the increased energy availability during this season as the main determinant of evapotranspiration rates.

Shuttleworth calibrated his model to fit observations at a particular site, and so it is instructive to review the results of subsequent field studies carried out at other locations in the Amazon Basin. Multiyear eddy covariance measurements at two sites in the Tapajos National

Corresponding author address: Hanan Karam, 15 Vassar St., 48-212, Cambridge, MA 02139.
E-mail: hnkaram@mit.edu

DOI: 10.1175/2008JHM888.1

Forest in eastern Amazonia (2.9°S, 54.9°W) produced strong evidence that evapotranspiration in this region is not water limited during the dry season, which has an average length of 5 months (months with total rainfall less than 100 mm; see Malhi et al. 2002) and about 30% of the wet-season rainfall rate (da Rocha et al. 2004; Saleska et al. 2003; Hutyra et al. 2007). In these old-growth forests, evapotranspiration consistently increased during the dry season, tracking net radiation and maintaining a constant evaporative fraction throughout the year (da Rocha et al. 2004; Hutyra et al. 2007). Furthermore, the total dry-season evapotranspiration consistently exceeded dry-season rainfall, in 1 yr by up to 80%, indicating that the trees had access to large reservoirs of water (da Rocha et al. 2004; Saleska et al. 2003; Hutyra et al. 2007). Soil moisture and sap flow measurements in these forests showed that trees extracted water from depths of at least 2 m, and that hydraulic redistribution by deep roots resulted in continuous replenishment of shallow soil water (da Rocha et al. 2004; Lee et al. 2005; Oliveira et al. 2005). More evidence of the importance of deep roots comes from another mature forest farther east, where Nepstad et al. (1994) used extensive soil moisture measurements to show that 75% of the water extracted from the soil during a severe 5.5-month-long dry season came from depths of 2–8 m, allowing trees to maintain an evapotranspiration rate approximately 6 times the rainfall rate. Eddy covariance data from another site in eastern Amazonia within the Caxiuana National Forest (1.7°S, 51.5°W) also showed increased evapotranspiration during the dry season in 1999, tracking net radiation and vapor pressure deficit. However, no information is available on the interannual variability of hydrologic fluxes at this site (Souza-Filho et al. 2005; Carswell et al. 2002).

Field studies in central Amazonia are not as conclusive with regard to the seasonal patterns of and controls on evapotranspiration. The climate in this region is wetter on average than in the eastern Amazon Basin, with a higher mean annual rainfall rate, and a shorter and milder dry season (Malhi et al. 2002; Araújo et al. 2002; Sombroek 2001). As mentioned above, two years of data collected at the Ducke Reserve near Manaus showed that evapotranspiration rates from this forest increased during the dry season along with potential evapotranspiration, indicating that the increase in stomatal resistance during this period was relatively minor (Shuttleworth 1988). However, data from a nearby forest in the Cuxeiras Reserve suggest that interannual variability in rainfall may be an important determinant of the seasonal evapotranspiration cycle in this region. While Malhi et al. (2002) found that transpiration decreased during the dry season in 1995/96, indicating water stress, Araújo et al. (2002) found that energy partitioning was constant over the dry and wet seasons in 1999/2000. The contradictory conclusions reached by these investigators may be explained by the fact that 1999/2000 was a La Niña year, and hence a much wetter year than 1995/96.

The results summarized thus far all originate from sites in close proximity to the equator. Werth and Avissar (2004) propose that a forest's distance from the equator may be an important determinant of the seasonality of its evapotranspiration rates, as it determines the phase and amplitude of the annual cycle of incident solar radiation. In fact, at the Jaru Biological Reserve in southwest Amazonia (10.1°S, 61.9°W), where eddy covariance measurements of evapotranspiration have been under way, net radiation reaches its maximum during the wet season (Juarez et al. 2007). Juarez et al. (2007) analyze three years of evapotranspiration and soil moisture data from this site and show that the rates of evapotranspiration peak during the wet season, but appear to track net radiation rather than rainfall: they are maintained at the rates of potential evapotranspiration during the dry season, sustained by deep soil moisture that is recharged during the subsequent wet season (Juarez et al. 2007; von Randow et al. 2004). These observations contrast with data from a nearby site that had been converted to pasture, and which experienced strong water limitation during the dry season (von Randow et al. 2004).

Perhaps the data point that most stands out in the literature is that presented by Vourlitis et al. (2002) describing measurements of evapotranspiration in a mature transitional forest in southeast Amazonia (11.4°S, 55.3°W). While the annual evapotranspiration cycles observed at other locations varied in phase, they all had relatively small amplitudes of 10%–20% of the mean annual value (Juarez et al. 2007). In contrast, Vourlitis et al. (2002) found that evapotranspiration in the transitional forest was highly seasonal, correlating with precipitation and increasing by 66% during the wet season, even in a wetter-than-average year.

The field studies reviewed above, though still limited in their coverage (e.g., there are no measurements from the western or northern regions of the basin), indicate that the evapotranspiration regime in the Amazon Basin is spatially variable. The types of land cover and land use, as well as the climate patterns of a region, particularly with regard to rainfall and solar radiation, seem to be important determinants of its annual evapotranspiration cycle (see also Werth and Avissar 2004; Juarez et al. 2007). Nevertheless, the field data strongly suggest that a significant portion of Amazonian forests

can access large reservoirs of water through deep roots and hydraulic redistribution, and hence do not experience water stress during the dry season (see also Nepstad et al. 1994). This conclusion is also reached by Huete et al. (2006), who analyze satellite multispectral images and find that photosynthetic capacity or "greenness" increases significantly during the dry season over much of the Amazonian forests. The deep roots and hydraulic redistribution capabilities that allow Amazonian trees access to large reservoirs of soil water are not incorporated in today's global-scale land surface models, and hence these models likely exaggerate dry-season water limitation in the Amazon Basin. In fact, Lee et al. (2005) found that incorporating hydraulic redistribution in the NCEP–NCAR land surface model increased simulated dry-season evapotranspiration in the Amazon forests by 40%.

As field data remain inadequate at this time to develop a representative land surface model for the Amazon Basin, we investigate another approach to estimating its dominant evapotranspiration patterns based on evaluating its atmospheric water budget. The advantage of this approach is that it avoids models and parameterizations of evapotranspiration, which remain unreliable as long as the controls on and conditions of transpiration in the Amazon forests are poorly understood. This water budget method can be applied at the monthly time scale, informing us about the seasonal patterns of evapotranspiration and hence shedding light on the underlying processes. We carry out the hydrological accounting at the basin scale because of the limited accuracy of the reanalysis-based atmospheric data used (see Karam and Bras 2008). Domain averaging of these data allows for the cancellation of random errors and smoothes out the significant spatial variability in climate and environment to distill the dominant temporal patterns in the basin's hydrology.

2. Methodology and datasets

The atmospheric water balance is given by

$$[dw/dt] = [C] + [\mathrm{ET}] - [P], \tag{1}$$

where the square brackets indicate spatial averaging over our control region: $[w]$ is the water vapor content of the atmospheric column overlying the control region (also known as total precipitable water), $[C]$ is the net convergence of atmospheric water vapor flux over this region, and $[P]$ and [ET] are spatially averaged precipitation and evapotranspiration, respectively.

The computation of monthly averages of $[C]$ using data from three atmospheric reanalyses—the NCEP–NCAR (NCEP-1) and NCEP–Department of Energy (DOE) (NCEP-2) reanalyses, and the 40-yr European Centre for Medium-Range Weather Forecasts (ECMWF) Re-Analysis (ERA-40)—was described in Karam and Bras (2008). As explained there, the control region used is the subbasin that outlets at Obidos, the farthest downstream gauging station on the Amazon River. This watershed constitutes 70% of the entire Amazon Basin, and hence its hydrology is representative of the dominant hydrological patterns in the basin. Its selection as our study region allows us to utilize the reliable river discharge data collected at the Obidos station to correct the bias errors in reanalysis-derived $[C]$ estimates (as was done in Karam and Bras 2008).

Monthly means of Amazon River discharge at the Obidos gauging station were kindly provided by Jacques Callede, who is affiliated with the Hydrology and Geochemistry of the Amazon (HyBAm) project through the French Institut de Recherches pour le Développement (IRD; Callede et al. 2002). Work by Callede et al. (2001, 2002) improved the state–discharge relationship for this station based on detailed and long-term discharge measurements using an acoustic Doppler current profiler. The resulting relationship reduced the mean dispersion between stage-derived discharge and directly measured discharge to 2.9%.

Data from the same three reanalyses are used to obtain alternative estimates of the tendencies in atmospheric water vapor content over our control region, $[dw/dt]$. In the cases of NCEP-1 and NCEP-2, total precipitable water w is calculated from their vertically resolved specific humidity data product,

$$w = \frac{P_s}{g}\int_0^1 q\, d\sigma, \tag{2}$$

where q is specific humidity, P_s is surface pressure, and σ is the terrain-following vertical coordinate used in these reanalyses (Kalnay et al. 1996). This computation is not necessary in the case of ERA-40, which provides users with analyses of total precipitable water distributed on its global Gaussian grid.

As our water budget analysis is carried out at the monthly time scale, the tendency term actually represents the net change in domain-averaged precipitable water over a month's duration, computed as in Trenberth and Guillemot (1998):

$$\left[\frac{\Delta w}{\Delta t}\right] = \frac{[w_f] - [w_i]}{N}, \tag{3}$$

where N is the number of days in a given month. Here w_f is w at the end of that month, equivalent to the average of w at 1800 UTC on the last day of that month

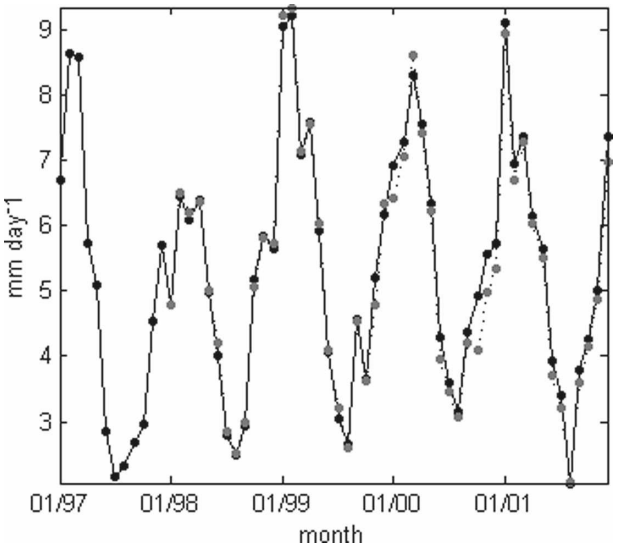

FIG. 1. Monthly [P] derived from the GPCP Combined Precipitation version 2 dataset (black circles) and the TRMM 3B43 version 5 dataset (gray circles). TRMM products are only available starting December 1997 and are plotted here starting January 1998.

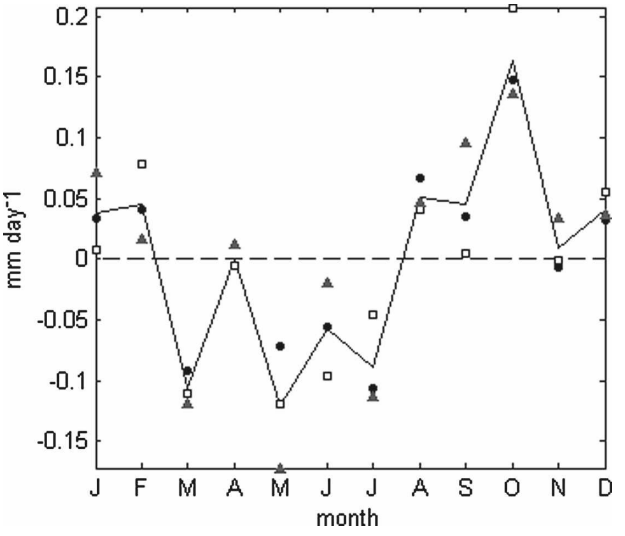

FIG. 2. Climatologies of monthly [$\Delta w/\Delta t$] derived from 1997–2001 time series, estimated using NCEP-1 data (black circles), NCEP-2 data (gray triangles), and ERA-40 data (white squares). Solid line is the average of estimates from the three reanalyses.

and at 0000 UTC on the first day of the following month; w_i, which is w at the beginning of that month, is similarly computed.

The Global Precipitation Climatology Project (GPCP) Combined Precipitation dataset (version 2) (Huffman et al. 1997) is used to obtain estimates of monthly [P]. A comparison of this dataset with the Tropical Rainfall Measuring Mission (TRMM) rainfall product 3B43 (version 5) (Adler et al. 2000; Kummerow et al. 2000) shows that their estimates of spatially averaged monthly rainfall for our control region agree closely (Fig. 1). This is expected since in both products, satellite-derived estimates of monthly rainfall are corrected for bias errors by adjusting their large-scale spatial averages (over $12.5° \times 12.5°$ boxes) to match Global Precipitation Climatology Center (GPCC) rain gauge data (Huffman et al. 1997; Adler et al. 2000). As we are averaging the precipitation products over an even larger area encompassing most of the Amazon Basin, the gauge data dominates our results from both the TRMM and GPCP datasets. Note, however, that these GPCC-based estimates fall at the lower end in the range of estimates of Amazonian rainfall given by various datasets, as shown by Costa and Foley (1998) and Marengo (2005), and will be discussed further in section 3b(1). [ET] remains the only unknown component in the atmospheric water budget for our subbasin, and it is computed as the residual of the water balance described by Eq. (1).

3. Results and discussion

a. Monthly tendencies in atmospheric water vapor content over the Amazon Basin

Rao et al. (1996) observed an increase in near-surface atmospheric humidity and vertically integrated atmospheric water vapor in central Brazil around the end of September, associated with the beginning of the rainy season. Li and Fu (2004) used data from the first generation ECMWF 15-yr reanalysis (ERA-15) to show that the transition to the wet season in the southern Amazon Basin begins with an increase in atmospheric moisture, which precedes the increase in rainfall rates by 25 days. In ERA-15, this increase in atmospheric water vapor is produced by increased latent heat flux in response to increasing net radiation at the surface (Li and Fu 2004).

Here we examine the monthly tendencies of total precipitable water over the Obidos subbasin to understand their seasonality and quantify their relative contribution to the hydrologic budget. Figure 2 presents the climatological annual cycle of [$\Delta w/\Delta t$], computed using data products from each of the three reanalyses covering the period 1997–2001. While there is significant spread in the alternative estimates of [$\Delta w/\Delta t$], the three reanalyses agree in their depiction of the seasonality of this storage term. Particularly, all three models show a reversal in the sign of the tendencies between February and March, and again between July and August.

In Fig. 3, the annual cycle of [$\Delta w/\Delta t$], an average of

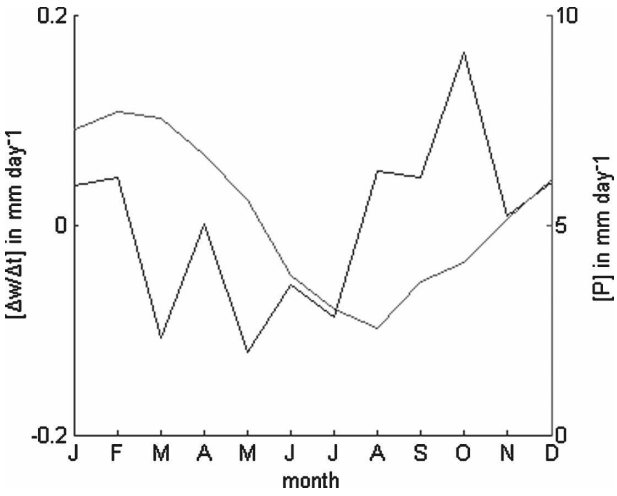

FIG. 3. Climatologies of monthly [P] based on the GPCP dataset (gray line, right-hand y axis) and monthly [$\Delta w/\Delta t$] computed by averaging estimates from the three reanalyses (black line, left-hand y axis). These climatologies are derived from time series covering 1997–2001.

results from the three reanalyses, is presented alongside that of precipitation. While the precipitation data imply that the rainy season begins in September following the August minimum in [P], [$\Delta w/\Delta t$] values indicate that the transition to the rainy season actually begins in August with a net increase in atmospheric water vapor during that month. Positive tendencies of total precipitable water are maintained through February, along with monotonously rising rainfall rates. The switch in sign of these tendencies in March, accompanied by a slight decline in [P], appears to mark the transition to the dry season.

As is evident from Fig. 3, the magnitude of monthly [$\Delta w/\Delta t$] is small compared to that of the other terms in our watershed's hydrologic budget. At its maximum in October, it remains less than 0.2 mm day^{-1} (average of results from the three reanalyses), 4% of the climatological precipitation rate for that month. Given the uncertainties in the other budget components, particularly [C], it is reasonable to neglect the contribution of this storage term to the monthly water balance.

b. *Amazonian evapotranspiration computed from the atmospheric water balance*

Spatially averaged evapotranspiration over the Obidos subbasin is computed as the residual of the atmospheric water balance equation, neglecting monthly tendencies in total precipitable water:

$$[\mathrm{ET}] = [P] - [C]. \tag{4}$$

Time series of monthly [C] covering the period September 1987 to August 2001, derived from each reanalysis, were bias corrected by Karam and Bras (2008) by matching their 14-yr mean to that of river discharge at Obidos. Following this correction, the remaining variability among alternative estimates of monthly [C] was attributed to random error in these time series. Karam and Bras (2008) quantified the random error associated with each reanalysis' [C] estimates at the annual time scale, using Obidos river discharge data as reference. For lack of additional information, we assume that these random error estimates provide an adequate measure of the relative accuracy of monthly [C] data derived from the different reanalyses. We then obtain a "best estimate" of monthly net atmospheric moisture flux convergence ([$\hat{C}$]) as a weighted average of the bias-corrected time series of [C] from the three reanalyses, where the weight factors are the inverses of the mean square errors computed by Karam and Bras (2008):

$$[\hat{C}] = 0.17[C]_{\mathrm{NCEP\text{-}1}} + 0.06[C]_{\mathrm{NCEP\text{-}2}} + 0.77[C]_{\mathrm{ERA\text{-}40}}. \tag{5}$$

As is evident from Eq. (5), ERA-40 was found to yield the most accurate estimates of [C], and hence contributes most to our best estimate of this variable.

Figure 4 presents monthly [ET] over the 14-yr period, derived from Eq. (4) using the GPCP precipitation rate and each of the alternative bias-corrected time series of [C] (from NCEP-1, NCEP-2, ERA-40, and the best estimate [$\hat{C}$]). It is clear that relying on different reanalyses to obtain data on atmospheric water vapor flux over the Amazon Basin leads one to very different depictions of temporal evapotranspiration patterns in the basin. As expected, the [ET] time series based on the best estimate [$\hat{C}$] follows closely that based on ERA-40-derived [C], with a small shift toward [ET] estimates computed using NCEP-1 data.

The monthly anomalies of [ET] relative to its climatological annual cycle, based on NCEP-1, NCEP-2, and ERA-40 time series of [C], are presented in Figs. 5a–c. The monthly [ET] estimates derived using NCEP-1 and NCEP-2 products exhibit a positive bias in the early to mid-1990s. This bias can be attributed to a drop in the [C] estimates from these reanalyses during this period, which was discussed by Karam and Bras (2008). It is probably artificial, as a corresponding bias does not show up in either the precipitation record or the river discharge data (Karam and Bras 2008).

1) MEAN ANNUAL [ET]

We compute an average annual [ET] value over our 14-yr study period of 2.1 mm day^{-1}. This result is actually independent of reanalysis-simulated atmospheric

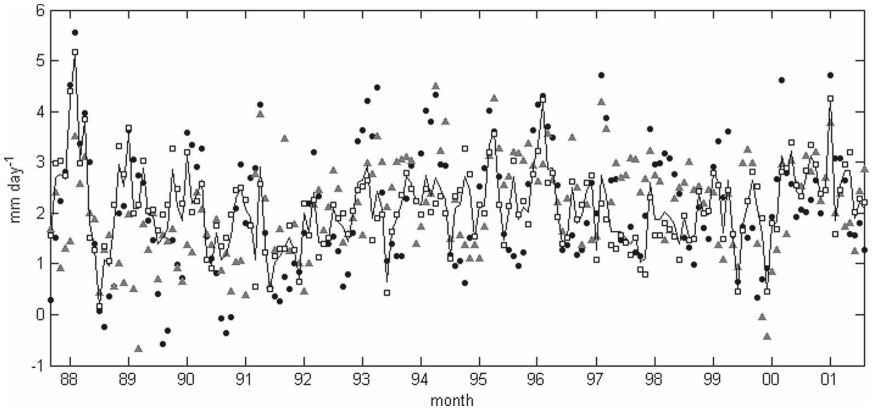

FIG. 4. Monthly [ET] for September 1987–August 2001, computed as the residual of the atmospheric water balance using [C] estimates from ERA-40 (white squares), NCEP-1 (black circles), NCEP-2 (gray triangles), and the best estimate [$\hat{C}$] (black line). Note that [ET] based on [$\hat{C}$] follows closely the ERA-40 based time series with a small shift toward the NCEP-1–based estimates.

moisture flux convergence. It is effectively produced by the difference between mean [P] and [R] for our study period, because the bias correction applied to [C] estimates matched their long-term average with that of river discharge.

The mean annual runoff rate that we computed for our subbasin is 3.1 mm day^{-1}, agreeing closely with other published values of Amazonian runoff. Zeng (1999) and Marengo (2005) calculate a mean annual runoff rate of 2.9 mm day^{-1} for the whole Amazon Basin, by extrapolating measured discharge at Obidos to estimate flow at the Amazon River's mouth. Roads' (2002) estimate of mean annual runoff over the entire basin is 3.2 mm day^{-1}, derived from the global gridded runoff dataset produced by Fekete et al. (2002).

The precipitation data used in our hydrological accounting are not as certain as the river discharge data. Marengo (2005) computes a mean annual basin-averaged rainfall rate of 5.2 mm day^{-1} for the period 1970–99 using GPCP data covering the whole Amazon Basin, matching our result for the Obidos subbasin and for the period 1988–2001. In comparison, he calculates a mean annual basin-averaged rainfall rate of 5.6 mm day^{-1} from the Climate Prediction Center (CPC) Merged Analysis of Precipitation (CMAP) global gridded dataset, 6.0 mm day^{-1} from the Climatic Research Unit (CRU) gauge-based global gridded dataset, and 5.8 mm day^{-1} starting from the raw rainfall records of 164 gauging stations. Similarly, Costa and Foley (1998) find that the GPCP dataset is negatively biased in its estimate of Amazonian rainfall compared to three datasets that are based exclusively on rain gauge data, and which produce a mean annual basin-averaged precipitation rate between 5.8 and 5.9 mm day^{-1}. Hence, the GPCP data used in our work may be negatively biased and would result in similarly biased estimates of evapotranspiration [see Eq. (4)].

However, this potential negative bias in GPCP data does not completely explain why our estimate of mean annual [ET] is significantly lower than most values of Amazonian evapotranspiration published in the literature (Table 1). Even if an alternative rainfall dataset had been used in our study, such as the CRU product, our result would still not exceed 3 mm day^{-1}. In comparison, estimates of mean annual basin-averaged

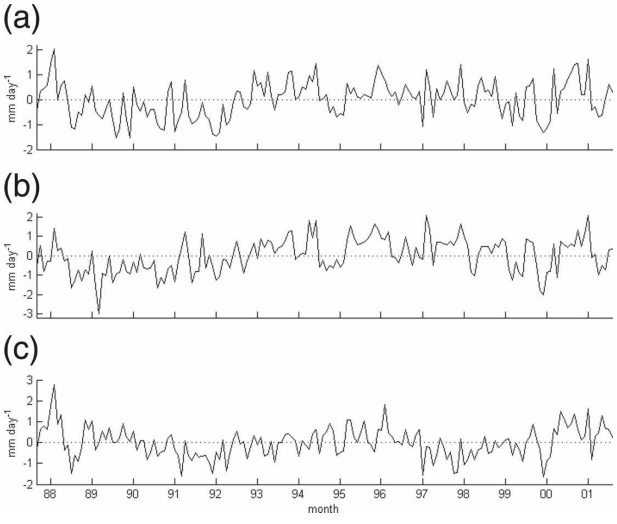

FIG. 5. (a) Monthly anomalies of [ET] based on [C] data derived from NCEP-1. The anomaly for each month is computed as the difference between [ET] for that month and climatological [ET] for that month over the period September 1987–August 2001. (b) As in (a), but with [C] data derived from NCEP-2. (c) As in (a), but with [C] data derived from ERA-40.

TABLE 1. Basin-scale evapotranspiration estimates for the Amazon Basin. Estimates from earlier publications are also provided in Costa and Foley (1999).

Source	Mean annual basin-scale evapotranspiration estimate (mm day^{-1})	Method and data sources	Time period covered by study
Rao et al. (1996)	4.5	Computed from the atmospheric water balance, using atmospheric data from once-daily ECMWF analyses and precipitation estimates from rain gauge records	1985–89
Costa and Foley (1997)	3.7	Simulated by the LSX land surface model, using atmospheric forcing data from observation-based datasets (climatological averages were used)	Five simulation years
Zeng (1999)	4.6	Derived from the NASA GEOS-1 reanalysis gridded evaporation product	1985–93
Costa and Foley (1999)	3.8	Computed from the terrestrial water balance, neglecting storage change, using precipitation and runoff estimates derived from the NCEP–NCAR reanalysis products	1976–96
Callede et al. (2002)	3.3	Computed from the terrestrial water balance using precipitation estimates from rain gauge data and runoff estimates from gauged discharge at the Obidos station	1969–1992
Marengo (2005)	4.3	Derived from the NCEP–NCAR reanalysis gridded evaporation product	1970–99
Betts et al. (2005)	3.5	Derived from the ERA-40 reanalysis gridded evaporation product	1958–2001
Ramillien et al. (2006)	~3.3	Computed as the residual of the terrestrial water balance applied at the monthly time scale, using GRACE-based estimates of monthly changes in land water mass	July 2002–June 2004

evapotranspiration produced by various land surface models range between 3.5 and 4.8 mm day^{-1} (Table 1; Betts et al. 2005; Marengo 2005; Costa and Foley 1997; Zeng 1999).

There are few publications that compute Amazonian evapotranspiration through an observation-based water balance analysis (see Table 1). Callede et al. (2002) evaluate the terrestrial hydrologic budget of the Obidos subbasin over the period 1970–92, assuming that the mean change in terrestrial water storage over this period is negligible. Using the same river discharge data that we rely upon, they obtain a mean annual runoff rate of 3.2 mm day^{-1}. They estimate mean annual rainfall from the records of 46 gauges to be 6.5 mm day^{-1}—much higher than our GPCP-based estimate of this field and probably biased upward because of the small number of gauges used. Their resulting estimate of mean annual domain-averaged evapotranspiration is 3.3 mm day^{-1}, still lower than published values of Amazonian evapotranspiration produced using land surface models. A more sound comparison can be made between our results and those of Ramillien et al. (2006), which are based on completely different datasets than used here. Ramillien et al.'s method is unique in that they analyze the terrestrial water budget of the Amazon Basin at the monthly scale, using data from the Gravity Recovery and Climate Experiment (GRACE) mission to estimate changes in terrestrial water storage. Their study covers a very limited time period, July 2002–June 2004, and so cannot be used to obtain an estimate of climatological evapotranspiration. Nevertheless, the mean basin-averaged evapotranspiration rate they derive over the first 12 months of their study period is ~3 mm day^{-1}, while the last 12 months in their study, July 2003–June 2004, have a mean rate closer to 3.5 mm day^{-1}. However, this latter result is influenced by an anomalously high estimate of 5.5 mm day^{-1} for March 2004, which is likely erroneous since all their other monthly estimates do not exceed 4 mm day^{-1}.

Two other studies listed in Table 1 apply a hydrologic budget approach to compute Amazonian evapotranspi-

ration, but the input data on which their results are based are of questionable accuracy (Table 1; Rao et al. 1996; Costa and Foley 1999). Rao et al. (1996) use the atmospheric water balance equation, employing estimates of net atmospheric moisture flux convergence derived from once-daily ECMWF analyses, without checking and correcting for bias errors in these estimates. Costa and Foley (1999) deduce evapotranspiration from the terrestrial water balance, but rely on the NCEP–NCAR reanalysis for estimates of rainfall and runoff. Reanalysis estimates of these fields are completely model-based and thus highly error prone (Kalnay et al. 1996). Both these studies obtain significantly higher estimates of mean annual basin-scale evapotranspiration than that reported here.

In conclusion, it appears that among published estimates of mean annual basin-scale evapotranspiration rates in the Amazon, those derived through observation-based water budget computations (a minority), including ours, are significantly lower than those produced by commonly used land surface models.

2) CLIMATOLOGICAL ANNUAL CYCLE OF [ET]

While the terrestrial water balance equation can be used to reliably estimate the mean rate of regional-scale evapotranspiration in the Amazon Basin over a period of several years, it cannot be applied at the monthly or even annual scale without knowledge of the change in terrestrially stored water in the basin over these smaller time scales. Until recently such information was not available. The GRACE satellite, launched in 2002, now fills this gap by providing data on the earth's gravity field, which can be used to estimate monthly variations in terrestrial water storage for areas of $\sim 10^6$ km^2 (Ramillien et al. 2006; Wahr et al. 2006). Yet, in comparison to a GRACE-based computation of monthly regional evapotranspiration, the atmospheric water balance method used here has a couple of notable advantages. The atmospheric and precipitation data on which it relies have been collected for several decades, and hence this method can provide information on historical evapotranspiration patterns and long-term trends in a region's hydrologic budget (Seneviratne et al. 2004). Furthermore, the scientific community's experience with reanalysis products, used in lieu of raw atmospheric observations, is relatively well developed since these products have been available since the 1980s and have been used in numerous hydrologic studies covering the globe.

We find that the reanalysis-derived estimates of [C] are the most uncertain input in computing the seasonal cycle of [ET] for our subbasin, as the various reanalyses produce very different annual cycles of [C]. In contrast,

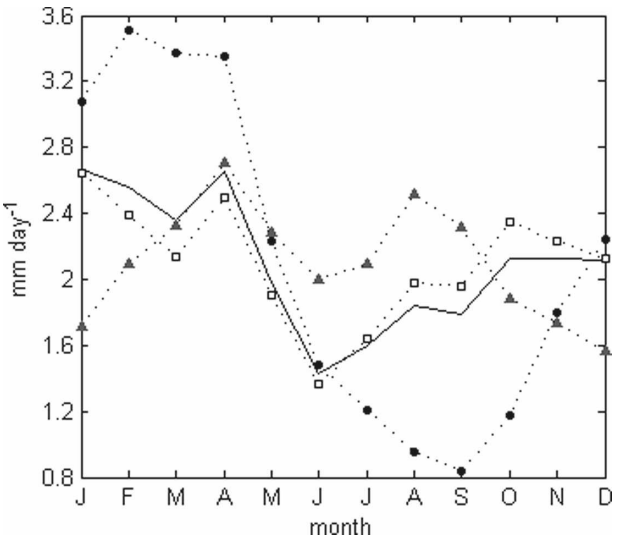

FIG. 6. Climatological annual cycles of [ET], based on [C] estimates derived from ERA-40 (white squares), NCEP-1 (black circles), NCEP-2 (gray triangles), and based on the best estimate [$\hat{C}$] (black line). Climatological averages are taken over the period September 1987–August 2001.

there is strong agreement among datasets on the basin-scale *seasonality* of Amazonian rainfall, despite the large range in estimates of mean annual precipitation from different sources. The annual cycle of [P] computed here using GPCP data matches closely the annual cycles of basin-averaged rainfall rates presented by Zeng (1999) based on the CMAP dataset and by Marengo (2005) based on the records of 164 gauging stations distributed over the Amazon Basin.

Figure 6 shows the climatological annual cycles of [ET] derived using [C] data from each of the three reanalyses, along with the result based on the best estimate [$\hat{C}$]. To clarify the source of the differences between the various [ET] cycles, Fig. 7 presents the mean annual cycle of [P] plotted alongside the alternative depictions of the annual cycle of [C]. Note that [ET] is computed as the difference between these two fields, as in Eq. (4). We also reproduce the plot by Werth and Avissar (2004) showing the annual cycles of spatially averaged surface net radiation over the Amazon Basin derived from four different datasets (Fig. 8). These datasets are carefully discussed by Werth and Avissar (2004). Our purpose is to get an idea of the seasonality of radiative forcing in the basin and its relationship to the seasonality of evapotranspiration, so it is enough to note that the various annual cycles plotted in Fig. 8 are in phase, particularly with regard to the June minimum. The annual maximum in net radiation is less certain, as two datasets show a pronounced peak in September–October while the other two show a flatter peak extending between September and March.

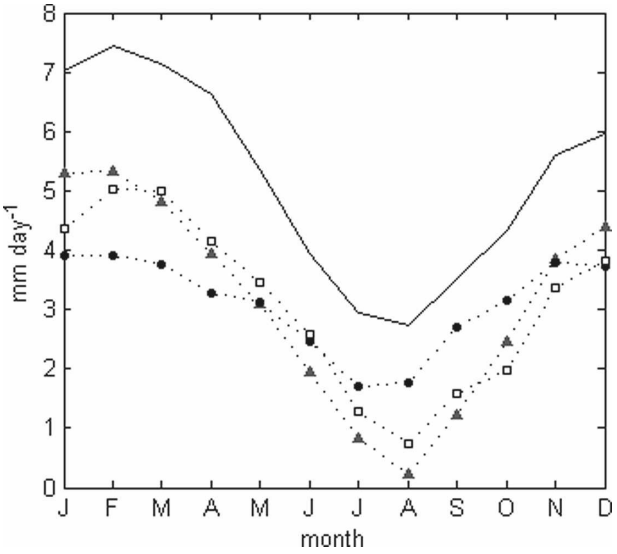

FIG. 7. Climatological annual cycles of [*P*] based on the GPCP dataset (solid line), and [*C*] derived from NCEP-1 (black circles), NCEP-2 (gray triangles), and ERA-40 (white squares). Climatological averages are taken over the period September 1987–August 2001.

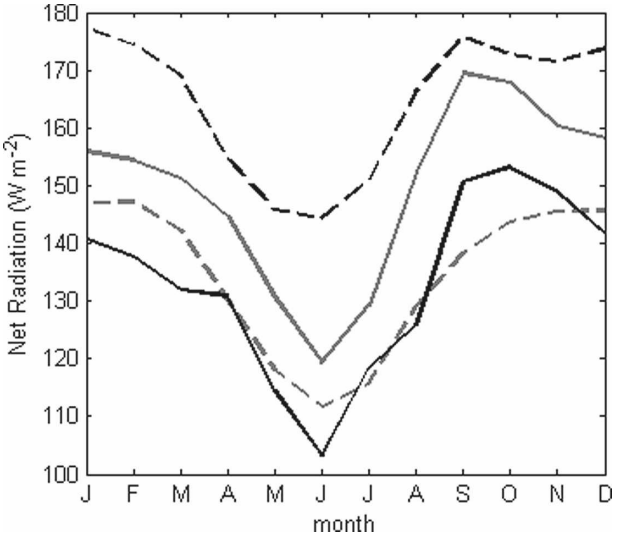

FIG. 8. Annual cycles of surface net radiation averaged over the Amazon Basin derived from the International Satellite Land Surface Climatology Project dataset (solid black line), simulated by the GISS Model II GCM (solid gray line) and produced by the NASA GEOS-1 reanalysis (dashed black line) and the NCEP–NCAR reanalysis (dashed gray line). Reproduced from Werth and Avissar (2004).

NCEP-1 based [ET] has a large seasonal variation of 3 mm day^{-1}, compared to the seasonal variation of approximately 1 mm day^{-1} obtained using ERA-40 and NCEP-2 data (Fig. 6). As can be seen in Fig. 7, this actually results from the relatively small seasonal variation in [*C*] modeled by NCEP-1, about 2.2 mm day^{-1}, compared to that modeled by ERA-40 and NCEP-2 (4.2 and 5 mm day^{-1}, respectively). Furthermore, the [ET] cycle computed using NCEP-1 data is in phase with basin-averaged rainfall, which along with its large seasonal variation would suggest that Amazonian evapotranspiration is highly water limited during the dry season.

In contrast, the annual cycle of [ET] based on ERA-40-derived [*C*], which is closely followed by that based on the best estimate [$\hat{C}$], tracks basin-averaged net radiation rather than precipitation (Figs. 6, 8). Both [ET] and average surface-incident radiation reach their minima in June, leading the rainfall minimum by 2 months, and proceed to rise rapidly during the two most severe months of the dry season. This suggests that evapotranspiration is predominantly energy limited in the Amazon Basin, with minimum transpiration being forced by a lack of energy availability rather than water availability. This conclusion is consistent with the small seasonal range in this [ET] cycle (1.3 mm day^{-1} compared to the range of 4.8 mm day^{-1} in [*P*]), which implies that Amazonian forests are buffered from the large seasonal variation in rainfall, most likely through moisture storage in the soil. It is more difficult to interpret the maximum in the ERA-40–based [ET] cycle, because it is not as pronounced as its minimum, and because the available datasets do not agree in their depiction of the peak in the annual cycle of surface net radiation over our study region (Fig. 8).

The [ET] cycle produced based on NCEP-2 estimates of [*C*] does not present a consistent picture with regard to the controls on evapotranspiration in the Amazon Basin. It does not agree with the scenario of water-limited transpiration, as its minimum occurs during the heart of the rainy season, and one of its two peaks occurs in August coinciding with the minimum in [*P*]. At the same time, it does not seem to be energy limited, as its minimum occurs during the period of peak radiation.

Following our analysis of the relative accuracy of data from each of the three reanalyses, we have the most confidence in the annual cycle of [ET] based on ERA-40 [*C*] estimates. Yet, this cycle differs from the climatological cycles of basin-averaged evapotranspiration produced by the land surface schemes of the NCEP–NCAR and NASA GEOS-1 reanalyses, both of which are in phase with precipitation (Zeng 1999; Werth and Avissar 2004; Marengo 2005). However, our result agrees with that of Huete et al. (2006), who show using Moderate Resolution Imaging Spectroradiometer (MODIS) satellite data that increased canopy greenness or photosynthetic activity during the dry season is prevalent throughout the Amazon Basin. Our results

also agree with those of Ramillien et al. (2006), who used GRACE data in a terrestrial water balance analysis, in that both show small seasonal variation in Amazonian evapotranspiration, on the order of 1 mm day^{-1}. However, Ramillien et al.'s study only covers two years, too short a period to derive a reliable picture of the basin's climatology.

3) COMPARISON TO EVAPOTRANSPIRATION SIMULATED BY THE REANALYSIS MODELS

We compare our estimate of the annual [ET] cycle, which we derived using ERA-40 [*C*] estimates in a water balance computation to that obtained from ERA-40 directly, simulated by the reanalysis' land surface scheme. At the time this paper was written, the climatological annual cycle of regional-scale evapotranspiration in the Amazon Basin simulated by ERA-40 had not been published in the peer-reviewed literature.

Monthly means of domain-averaged evapotranspiration simulated by the ERA-40 land surface model for the various subbasins of the Amazon were kindly provided by A. K. Betts (Betts et al. 2005). We computed the area-weighted average of these data for the Madeira, Solimoes, Negro, and Purus subbasins, which together constitute about 93% of the Obidos subbasin used in our water balance analysis. This domain was chosen because of the constraints imposed by the definition of subbasins in the Betts et al. (2005) dataset. Figure 9 presents the climatological annual cycle of this ERA-40-simulated [ET], calculated using monthly values from 1986 to 2001, alongside our estimate of the annual [ET] cycle computed using ERA-40 estimates of [*C*] through the atmospheric hydrologic budget approach.

The ERA-40-simulated [ET] and the [ET] estimates computed here through the water balance equation are not entirely independent, since they both incorporate a dependence on ERA-40-simulated atmospheric water vapor flux convergence. However, a correlation between these two estimates of [ET] cannot be expected a priori for two reasons: 1) the ERA-40-simulated water cycle is not closed, and its associated water balance equation includes a "residual term," which is produced by the aggregate effects of the analysis increments that are applied to the various hydrometeorological variables evaluated by ERA-40 (Betts et al. 2006; Roads et al. 2003); and 2) we do not rely on ERA-40-simulated rainfall in our water balance computation, but on the independent GPCP dataset.

It is evident that ERA-40's land surface scheme produces much higher values of Amazonian evapotranspiration than are obtained from our hydrologic budget analysis (Fig. 9). This result is consistent with the large

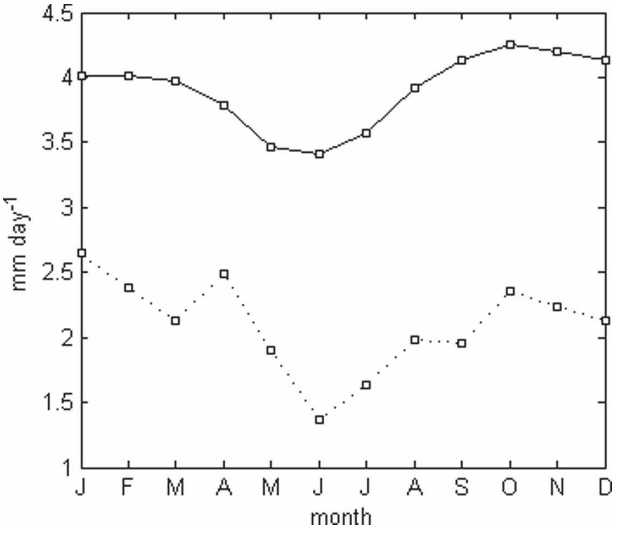

FIG. 9. Climatological annual cycles of [ET] computed as the residual of the atmospheric water balance using [*C*] estimates derived from ERA-40 (dotted line) and simulated by the land surface scheme of ERA-40 (solid line). Domain-averaged evapotranspiration rates simulated by the ERA-40 land surface model for the various subbasins of the Amazon were kindly provided by A. K. Betts (see text).

negative bias identified in ERA-40 [*C*] estimates by comparing them to river discharge data, provided that the reanalysis' water balance residual for the Amazon Basin is small relative to this bias (see Roads et al. 2003). The phases of the two [*ET*] cycles plotted in Fig. 9 show a key common feature. Both reach their minimum in June, coinciding with the minimum in surface net radiation and preceding the rainfall minimum, suggesting that Amazonian evapotranspiration is, for the most part, not water limited during the dry season.

In contrast, the seasonal cycle of basin-averaged evapotranspiration modeled by the NCEP–NCAR reanalysis tracks the seasonal variation of basin-averaged rainfall, implying that Amazonian evapotranspiration is water limited during the dry season: it is at its minimum despite the increase in net radiation during this season (Werth and Avissar 2004; Marengo 2005).

Hence, there is a fundamental difference between the land surface schemes of ERA-40 and the NCEP–NCAR reanalysis, in that the former simulates a larger reservoir of soil water that is replenished during the wet season and from which trees can extract water for transpiration during the dry season. In fact, the NCEP–NCAR and NCEP–DOE land surface schemes have two soil layers extending to a total depth of 1 m (Pan and Mahrt 1987; Kalnay et al. 1996; Betts et al. 2006), while the ERA-40 land surface model uses four soil layers extending to a depth of 1.89 m (Viterbo and Beljaars 1995). Furthermore, the latter model is signifi-

cantly more complex than that used in the NCEP reanalyses, and allows more spatial variability in soil and vegetation properties, including rooting depths (Van den Hurk et al. 2000; Betts et al. 2005, 2006).

Nevertheless, despite these differences between the reanalyses in their simulation of trees' access to soil moisture, they produce very similar and apparently high mean annual evapotranspiration rates (see Table 1). This highlights that the other parameterizations of the land surface models, besides the size of the soil moisture reservoir and the rooting depths, must be examined to explain these elevated evapotranspiration rates.

4. Conclusions

Spatially averaged evapotranspiration in the Obidos subbasin was computed at the monthly time scale for the period 1988–2001, as the residual of this watershed's atmospheric water balance. Input data include estimates of domain-averaged atmospheric moisture flux convergence derived from NCEP-1, NCEP-2, and ERA-40, and precipitation from the GPCP dataset. River discharge measurements collected at the Obidos gauging station on the Amazon River were used to correct bias errors in the reanalysis-derived estimates of $[C]$. Monthly tendencies in atmospheric water vapor content over our domain, computed using reanalysis data, were found to be of negligible magnitude compared to $[P]$ and $[C]$.

Annual mean [ET] during our study period was found to be 2.1 mm day^{-1}. This estimate is completely dependent on the river discharge and rainfall data, since the full-length averages of the $[C]$ time series from all three reanalyses were adjusted to match average runoff. While our result could be revised upward by using alternative datasets of Amazonian rainfall, it would still not exceed 3 mm day^{-1}. A comparison to other published estimates of mean annual Amazonian evapotranspiration indicates that our result is significantly lower than those produced by a variety of land surface models, which range between 3.5 and 4.5 mm day^{-1}. Estimates based on observations seem to be more consistent with our results but few are available.

At the monthly time scale, the main source of uncertainty in our [ET] estimates lies in the reanalysis-based time series of net atmospheric moisture flux convergence over our control region. Estimates of this field produced by ERA-40 were found to be significantly more accurate at the annual time scale than those produced by NCEP-1 and NCEP-2 (Karam and Bras 2008). Thus, they dominate the derived "best estimate" $[\hat{C}]$, which was computed as a weighted average of the alternative time series of $[C]$. Our best estimate of the climatological annual cycle of [ET] was compared to the cycles of rainfall and surface net radiation to deduce the prevalent conditions of transpiration in the Amazon Basin.

Since [ET] in this work is computed by subtracting time series of $[P]$ and $[C]$, it is sensitive to errors in the monthly estimates of $[P]$ and $[C]$. Spatial averaging (over the Obidos subbasin) and temporal averaging (over the 14-yr period) reduce the uncertainty in our results. The most certain feature in the annual cycle of [ET] presented here is its small variability compared to the seasonal variation of rainfall in the Amazon Basin. Another prominent feature of this cycle is its minimum in June, which coincides with the minimum in basin-averaged surface net radiation, suggesting that energy limitation is the predominant control on Amazonian evapotranspiration. This result agrees with the conclusion of Huete et al. (2006), based on time-lapse satellite images of canopy greenness. However, our result contradicts those of several land surface models that simulate annual cycles for evapotranspiration that are in phase with rainfall. The main problem with these land surface models is likely that they underestimate the depth to which Amazonian trees can extract water, as suggested by our comparison of the basin-scale evapotranspiration cycles produced by the land surface schemes of ERA-40 and NCEP-1.

The water balance analysis carried out here would greatly benefit from better information on the quality of reanalysis-produced data on net atmospheric moisture flux convergence over the Amazon Basin, particularly at the monthly time scale, which is lacking in the literature (Trenberth et al. 2001). There is also much need for algorithms that can be used to extract such information, particularly for regions where radiosonde observations are scarce.

As a final note, our study joins several others in emphasizing the importance of testing and revising available hydrological and land surface models for the Amazon forests, using observation-based data to verify these models' results both at local and regional scales.

Acknowledgments. Grant funding from TRMM/NASA, NAG5-13638, and NNG06GD63G supported this work. The Ferret program was used for data analysis and some graphics production. Ferret is a product of NOAA's Pacific Marine Environmental Laboratory. Information is available online (http://ferret.pmel.noaa.gov/Ferret/). We are grateful to Dr. JingFeng Wang for his comments and revisions during the writing process. We gratefully acknowledge the use of the ERA-0 river basin dataset (Betts et al. 2003a,b, 2005), provided to us

by A. K. Betts. We are also very thankful to the three anonymous reviewers who helped improve the content and presentation of this study.

REFERENCES

Adler, R. F., G. J. Huffman, D. T. Bolvin, S. Curtis, and E. J. Nelkin, 2000: Tropical rainfall distributions determined using TRMM combined with other satellite and rain gauge information. *J. Appl. Meteor.,* **39,** 2007–2023.

Araújo, A. C., and Coauthors, 2002: Comparative measurements of carbon dioxide fluxes from two nearby towers in a central Amazonian rainforest: The Manaus LBA site. *J. Geophys. Res.,* **107,** 8090, doi:10.1029/2001JD000676.

Betts, A. K., J. H. Ball, M. Bosilovich, P. Viterbo, Y. Zhang, and W. B. Rossow, 2003a: Intercomparison of water and energy budgets for five Mississippi subbasins between ECMWF reanalysis (ERA-40) and NASA Data Assimilation Office fvGCM for 1990–1999. *J. Geophys. Res.,* **108,** 8618, doi:10.1029/2002JD003127.

——, ——, and P. Viterbo, 2003b: Evaluation of the ERA-40 surface water budget and surface temperature for the Mackenzie River basin. *J. Hydrometeor.,* **4,** 1194–1211.

——, ——, ——, A. G. Dai, and J. Marengo, 2005: Hydrometeorology of the Amazon. *J. Hydrometeor.,* **6,** 764–774.

——, M. Zhao, P. A. Dirmeyer, and A. C. M. Beljaars, 2006: Comparison of ERA40 and NCEP/DOE near-surface data sets with other ISLSCP-II data sets. *J. Geophys. Res.,* **111,** D22S04, doi:10.1029/2006JD007174.

Callede, J., P. Kosuth, and E. de Oliveira, 2001: Establishment of the stage-discharge relationship of the River Amazon at Obidos: Normal difference in level method using variable geometry. *Hydrol. Sci. J.,* **46,** 451–463.

——, J. L. Guyot, J. Ronchail, M. Molinier, and E. De Oliveira, 2002: The River Amazon at Obidos (Brazil): Statistical studies of the discharges and water balance. *Hydrol. Sci. J.,* **47,** 321–333.

Carswell, F. E., and Coauthors, 2002: Seasonality in CO_2 and H_2O flux at an eastern Amazonian rain forest. *J. Geophys. Res.,* **107,** 8076, doi:10.1029/2000JD000284.

Costa, M. H., and J. A. Foley, 1997: Water balance of the Amazon Basin: Dependence on vegetation cover and canopy conductance. *J. Geophys. Res.,* **102** (D20), 23 973–23 989.

——, and ——, 1998: A comparison of precipitation datasets for the Amazon basin. *Geophys. Res. Lett.,* **25,** 155–158.

——, and ——, 1999: Trends in the hydrologic cycle of the Amazon basin. *J. Geophys. Res.,* **104,** 14 189–14 198.

da Rocha, H., M. L. Goulden, S. D. Miller, M. C. Menton, L. D. V. O. Pinto, H. C. de Freitas, and A. M. E. Figueira, 2004: Seasonality of water and heat fluxes over a tropical forest in eastern Amazonia. *Ecol. Appl.,* **14,** S22–S32.

Fekete, B. M., C. J. Vörösmarty, and W. Grabs, 2002: High-resolution fields of global runoff combining observed river discharge and simulated water balances. *Global Biogeochem. Cycles,* **16,** 1042, doi:10.1029/1999GB001254.

Huete, A. R., and Coauthors, 2006: Amazon rainforests green-up with sunlight in dry season. *Geophys. Res. Lett.,* **33,** L06405, doi:10.1029/2005GL025583.

Huffman, G. J., and Coauthors, 1997: The Global Precipitation Climatology Project (GPCP) combined precipitation dataset. *Bull. Amer. Meteor. Soc.,* **78,** 5–20.

Hutyra, L. R., and Coauthors, 2007: Seasonal controls on the exchange of carbon and water in an Amazonian rain forest. *J. Geophys. Res.,* **112,** G03008, doi:10.1029/2006JG000365.

Juarez, R. I. N., M. G. Hodnett, R. Fu, M. L. Goulden, and C. von Randow, 2007: Control of dry season evapotranspiration over the Amazonian Forest as inferred from observations at a southern Amazon forest site. *J. Climate,* **20,** 2827–2839.

Kalnay, E., and Coauthors, 1996: The NCEP/NCAR 40-Year Reanalysis Project. *Bull. Amer. Meteor. Soc.,* **77,** 437–471.

Karam, H. N., and R. L. Bras, 2008: Estimates of net atmospheric moisture flux convergence over the Amazon basin: A comparison of reanalysis products. *J. Hydrometeor.,* **9,** 1035–1047.

Kummerow, C., and Coauthors, 2000: The status of the Tropical Rainfall Measuring Mission (TRMM) after two years in orbit. *J. Appl. Meteor.,* **39,** 1965–1982.

Lee, J. E., R. S. Oliveira, T. E. Dawson, and I. Fung, 2005: Root functioning modifies seasonal climate. *Proc. Natl. Acad. Sci. USA,* **102,** 17 576–17 581.

Li, W., and R. Fu, 2004: Transition of the large-scale atmospheric and land surface conditions from the dry to the wet season over Amazonia as diagnosed by the ECMWF Re-Analysis. *J. Climate,* **17,** 2637–2651.

Malhi, Y., E. Pegoraro, A. D. Nobre, M. G. P. Pereira, J. Grace, A. D. Culf, and R. Clement, 2002: Energy and water dynamics of a central Amazonian rain forest. *J. Geophys. Res.,* **107,** 8061, doi:10.1029/2001JD000623.

Marengo, J. A., 2005: Characteristics and spatio-temporal variability of the Amazon River Basin Water Budget. *Climate Dyn.,* **24,** 11–22.

Nepstad, D. C., and Coauthors, 1994: The role of deep roots in the hydrological and carbon cycles of Amazonian forests and pastures. *Nature,* **372,** 666–669.

Oliveira, R. S., T. E. Dawson, S. S. O. Burgess, and D. C. Nepstad, 2005: Hydraulic redistribution in three Amazonian trees. *Oecologia,* **145,** 354–363.

Pan, H. L., and L. Mahrt, 1987: Interaction between soil hydrology and boundary-layer development. *Bound.-Layer Meteor.,* **38,** 185–202.

Ramillien, G., F. Frappart, A. Güntner, T. Ngo-Duc, A. Cazenave, and K. Laval, 2006: Time variations of the regional evapotranspiration rate from Gravity Recovery and Climate Experiment (GRACE) satellite gravimetry. *Water Resour. Res.,* **42,** W10403, doi:10.1029/2005WR004331.

Rao, V. B., I. F. A. Cavalcanti, and K. Hada, 1996: Annual variation of rainfall over Brazil and water vapor characteristics over South America. *J. Geophys. Res.,* **101,** 26 539–26 552.

Roads, J., 2002: Closing the water cycle. *GEWEX News,* No. 12, International GEWEX Project Office, Silver Spring, MD, 1–8.

——, and Coauthors, 2003: GCIP water and energy budget synthesis (WEBS). *J. Geophys. Res.,* **108,** 8609, doi:10.1029/2002JD002583.

Saleska, S. R., and Coauthors, 2003: Carbon in Amazon Forests: Unexpected seasonal fluxes and disturbance-induced losses. *Science,* **302,** 1554–1557.

Seneviratne, S. I., P. Viterbo, D. Lüthi, and C. Schär, 2004: Inferring changes in terrestrial water storage using ERA-40 ReAnalysis data: The Mississippi River basin. *J. Climate,* **17,** 2039–2057.

Shuttleworth, W. J., 1988: Evaporation from Amazonian rainforest. *Proc. Roy. Soc. London,* **233,** 321–346.

Sombroek, W., 2001: Spatial and temporal patterns of Amazon rainfall. *AMBIO J. Hum. Environ.,* **30** (7), 388–396.

Souza-Filho, J. D. C., A. Ribeiro, M. H. Costa, and J. C. P. Cohen,

2005: Control mechanisms of the seasonal variation of transpiration in a northeast Amazonian tropical rainforest (in Portuguese). *Acta Amazonica,* **35** (2), 223–229.

Trenberth, K. E., and C. J. Guillemot, 1998: Evaluation of the atmospheric moisture and hydrological cycle in the NCEP-NCAR reanalyses. *Climate Dyn.,* **14,** 213–231.

——, D. P. Stepaniak, J. W. Hurrell, and M. Fiorino, 2001: Quality of reanalyses in the Tropics. *J. Climate,* **14,** 1499–1510.

Van den Hurk, B. J. J. M., P. Viterbo, A. C. M. Beljaars, and A. K. Betts, 2000: Offline validation of the ERA-40 surface scheme. ECMWF Tech. Memo. 295, 43 pp. [Available online at http://www.ecmwf.int/publications/library/ecpublications/_pdf/tm/001-300/tm295.pdf.]

Viterbo, P., and A. C. M. Beljaars, 1995: An improved land surface parameterization scheme in the ECMWF model and its validation. *J. Climate,* **8,** 2716–2748.

von Randow, C., and Coauthors, 2004: Comparative measurements and seasonal variations in energy and carbon exchange over forest and pasture in South West Amazonia. *Theor. Appl. Climatol.,* **78,** 5–26.

Vourlitis, G. L., N. Priante Filho, M. M. S. Hayashi, J. D. Nogueira, F. T. Caseiro, and J. H. Campelo Jr., 2002: Seasonal variations in the evapotranspiration of a transitional tropical forest of Mato Grosso, Brazil. *Water Resour. Res.,* **38,** 1094, doi:10.1029/2000WR000122.

Wahr, J., S. Swenson, and I. Velicogna, 2006: Accuracy of GRACE mass estimates. *Geophys. Res. Lett.,* **33,** L06401, doi:10.1029/2005GL025305.

Werth, D., and R. Avissar, 2004: The regional evapotranspiration of the Amazon. *J. Hydrometeor.,* **5,** 100–109.

Zeng, N., 1999: Seasonal cycle and interannual variability in the Amazon hydrologic cycle. *J. Geophys. Res.,* **104,** 9097–9106.